Basic Dose Response of Fluorescent Screen-based Potal Imaging Device

Inhwan J. Yeo, Ph. D. *, Yonas Yohannes, M. S. †, and Yunping Zhu, Ph. D. †

*Department of Radiation Oncology, Samsung Medical Center, College of Medicine,
Sung Kyun Kwan University, Seoul, Korea
†Department of Radiation Oncology, St.Jude Children's Research Hospital, Memphis, USA

Purpose : The purpose of this study is to investigate fundamental aspects of the dose response of fluorescent screen-based electronic portal imaging devices (EPIDs).

Materials and Methods : We acquired scanned signal across portal planes as we varied the radiation that entered the EPID by changing the thickness and anatomy of the phantom as well as the air gap between the phantom and the EPID. In addition, we simulated the relative contribution of the scintillation light signal in the EPID system

Results : We have shown that the dose profile across portal planes is a function of the air gap and phantom thickness. We have also found that depending on the density change within the phantom geometry, errors associated with dose response based on the EPID scan can be as high as 7%. We also found that scintillation light scattering within the EPID system is an important source of error.

Conclusion : This study revealed and demonstrated fundamental characteristics of dose response of EPID, as relative to that of ion chambers. This study showed that EPID based on fluorescent screen cannot be an accurate dosimetry system.

Key Words : Portal dosimetry, Electronic portal imaging device (EPID), Light scattering

INTRODUCTION

Portal dosimetry can be perfomed by using detectors such as electronic portal imaging devices (EPIDs)[1~8] and x-ray film.[9~12] Because its objective is to verify dose delivery in radiotherapy treatment, portal dosimetry must be performed within an acceptable margin of error. However, only a few previous studies quantitatively measured the dose profile across the portal plane.[2,7,11,12] The current research trend of real-time dosimerty eliminates x ray film as a candidate dosimeter. In addition, despite the accuracy of ion-chamber matrices based EPID,[7] its disadvantages regarding portal dosimetry include a relatively long measurement time, high cost, and poor spatial resolution Little portal dosimetry work has been done with fluorescent screen-based EPIDs, but they seem to be and attractive alternative fo portal dosimetry

(two-dimensional measurement).[2]

Most currently available EPIDs use fluorescent screens that contain high-Z (i.e., atomic number) elements such as gadolinium. These screens are the primary media sensitive to incoming radiation, and their response characteristics determine those of the devices. The high-Z element in the screen makes EPIDs sensitive to low-energy photons (i.e., energy less than 400 KeV) transmitted through the patient, thereby improving the response (i.e., signal and contrast) of the detectors as imaging devisces. However, the presence of the high-Z element becomes undesirable for dosimetry applications because the response of an ideal dosimeter is equivalent to that of tissue[13] : tissue is less sensitive to low-energy photons than are EPIDs. More specifically, photon fluence spectra (i.e., relative abundance of the low-energy photons in the spectra) vary across portal planes, and their variance is also a function of patient thickness and the air gap between the patient and the EPID. We need to address the basis for this variation between the response of EPIDs and that of ion-chamber scanning if we are to use the EPID as a

Two-dimensional (2D) dosimeter. The findings of Jaffray et al. [14] rearding the scatter-to-primary photon ratio at beam axis on portal planes may not be directly extended to 2D dose profiles across portal planes.

The work of Heijman et al. [2] brings up another important factor regarding the response of the fluorescent screen-based EPIDs. Compared to ion-chamber scanning, use of an EPID led to a 6-7% error, which the authors attrivuted solely to light scattering through the optical chain (including the mirrors), in the system near the beam axis. We feel that energy-dependent characteristics of the EPID as well as light scattering contributed to the reported error. In the present study, we attempted to separately verify the problem of light scattering and to demonstrate the energy-dependent nature of the EPID response.

MATERIALS AND METHODS

We used the Philips (now Elekta, Shelton, CT) EPID, the SRI-100 system, and acquired images by using a procedure that we adopted in the macro command language that comes with the system. Our procedure is similar to those used by Kirby et al. [9] for portal
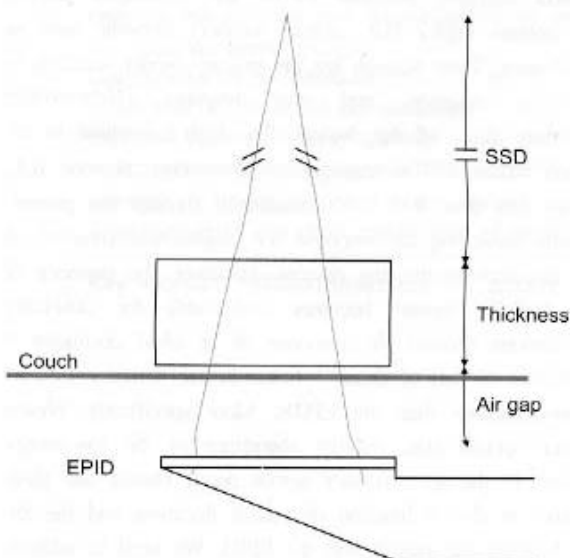

Fig. 1. EPID setup. The phantom on the couch is under the beam. The EPID fluorescent screen collects transmitted and scattered radiation.

dosimetry studies. To operate the EPID at the optimal signal-to-noise ratio, we optimized gain and camera offset. We also adjusted accu_var (the number of images acquired on the CCD chip in the system) and scan_var (the number of frames in the frame processor). For ion chamber scanning, we used the Wellhofer 700 system (Wellhofer North America, Barlett, TN).

To invesigate the effect of changing the air gap between the phantom and the EPID on the EPID response, we maintained the phantom thickness at 30 cm, the source-to-EPID (i.e. fluorescent layer) distance is fixed at 161.9 cm because the EPID is mounted on limac gantry. We then varied the air gap and source to (phantom) surface distance (SSD): when the air gap was 40 cm, the SSD was 91.9 cm; for a gap of 30 cm, the SSD was 101.9 cm, and for a gap of 20, the SSD was 111.9 Fig. 1 illustrates the EPID setup. For scanning with ion chamber, the phantom was mounted on a hollow table and then placed in a water tank (Fig. 2).

Next, ion chamber in the tank was maintained between 2 cm build-up water and 2 cm back-up water (including 1 cm water wquivalent tank bottom). We lowered the couch to maintain the source-to-ion chamber distance to be the same as the source-to-EPID distance at approximately 161.9 cm. By adjusting table-leg height, we reproduced the conditions of the EPID setup (I.E. SSD and air gap combinations).

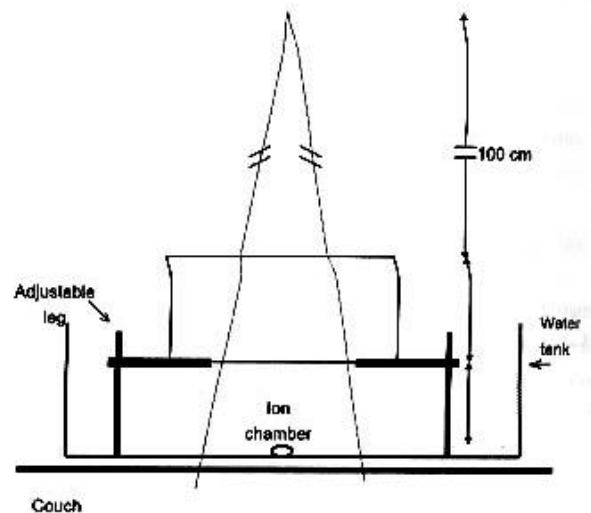We also investigated whether changing the thickness of the phantom affected EPID response. We

Fig. 2. Ion chamber setup. Phantom, table, and water tank are placed on the couch. X = air gap.

used a constant air gap of 30 cm then varied the SSD and the thickness of the phantom accordingly. The SSD was 101.9cm for the phantom thickness of 30 cm, 106.9 cm for a 25 cm phantom; 111.9cm for a phantom of 20 cm, 116.9cm for a 15 cm phantom,121.9cm for a thickness of 10cm,and 126.9cm for a phantom 5cm thick.

The above two investigations were performed to understand the fundamental dosimetric response of the EPID. To quantitatively estimate the accuracy associated with the EPID response for clinical situations, we used two types of heterogeneous phantoms, which are designed to produce large contrast by using combinations of lung and solid water materials. In this group of experiments, we used an air gap of 46.9 cm, a fixed SSD of 100cm, a 6 MV beam from the Philips SL-25 linac, and a 20 cm X 20 cm field. The relatively low energy/large field combination was appropriate for investigating the effect of scatter (i.e., detecting both scattered x-ray and scintillation light photons.) In addition, in an attempt to filter out the low-energy scattered component,[15,16] we placed a 0.4 mm thick lead filter on top of the EPID touch guard. For comparison, we used Kodak XV films sandwiched between 2 cm build-up and 2 cm back-up phantoms (this simulates the ion-chamber setup).[15,16] We tried to maintain the film at the same source-to-detector distance as that for the ion chamber and EPID.

We also investigated the relative contribution of scintillation light scatter within the EPID system in
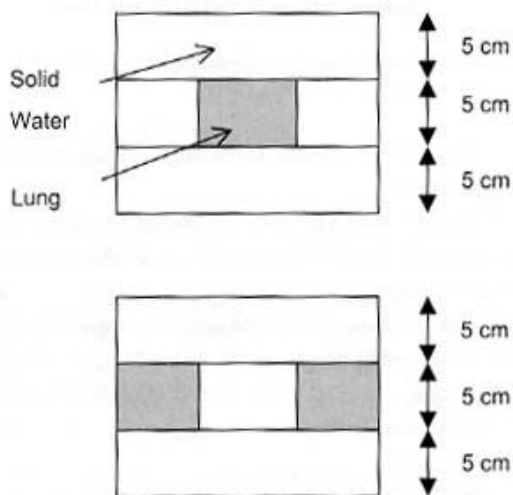
terms of its contribution to the signal outside of penumbra in addition to verify Heigiman et al's data on the beam central axis.[2] We used a 0.6cm thick white polystyrene plate in place of the original stainless steel cover on the EPID. Different sized light fields (from 5 X 5 cm² to 20 X 20 cm²) as defined by the multileaf collimator were then shined onto the plate with the room lights off and the CCD camera in the EPID then captured the signals after the background subtraction. We recorded the average pixel value within a region of interest(ROI) of 1 X 1 cm² on the central axis. Appropriate gain and light attenuation filter(placed on top of the white polystyrene plate) were used to avoid signal saturation. This setup simulated the scintillation signal on the central axis produced by the EPID without the possible energy-dependent nature of the EPID response. In addition, the relative pixel values(normalized to the central axis) scanned across a field of 20 X 20 cm² from both the light field and the EPID field (without solid water phantom in the beam) were analyzed and compared. The purpose was to find out if the over response outside the field is mainly due to the light scatter.

RESULTS

The results of this study can be summarized as follows.

Fig. 4 through 6 show that as the air gap increases, the curves between the two penumbra regions flatten(for EPID and ion chambers, respectively); the

Fig. 3. Heterogeneous phantoms used in this study. Phantom size (40 cm×40 cm) is large enough for the 20 cm×20 cm² x-ray field.
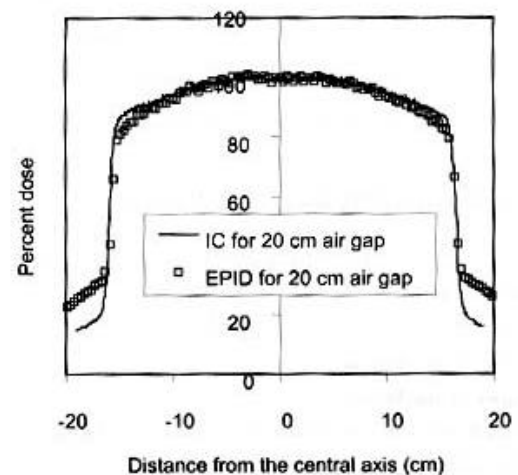

Fig. 4. EPID (squares) and ion-chamber (line) scans for a homogeneous phantom at an air gap of 20 cm.
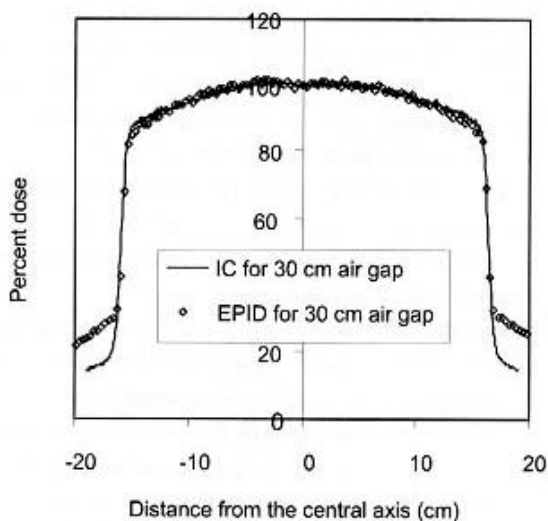
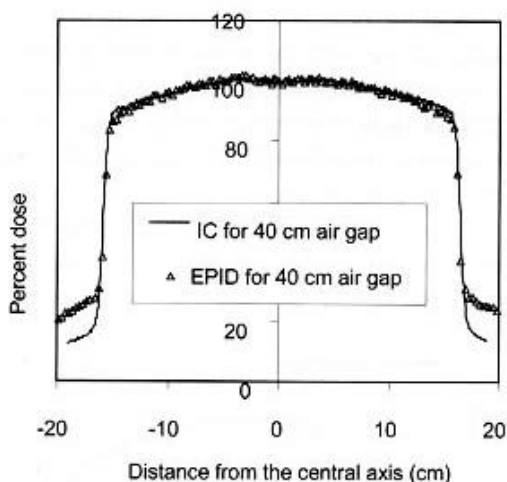Fig. 5. EPID (diamonds) and ion-chamber (line) scans for a homogeneous phantom at an air gap of 30 cm.

Fig. 6. EPID (triangles) and ion-chamber (line) scans for a homogeneous phantom at an air gap of 40 cm.

Fig. 7. The relative pixel values (normalized to the central axis) scanned across a field of 20×20 cm² from both the EPID field (line) and the light field (circles).

Fig. 8. EPID (diamonds) and ion-chamber (line) scans for a 5 cm-thick homogeneous phantom.

data in these figures were normalized at beam axis.

Fig. 4 through 6 show that outside the penumbra, the EPID data is always greater than ion-chamber data. Further, between the penumbrae, the data obtained by using the EPID are more curved than those for the ion chamber.

Fig. 7 shows the relative pixel values (normalized to the central axis) scanned across a field of 20 X 20 cm² from both the light field and the EPID field (without solid water phantom in the beam).

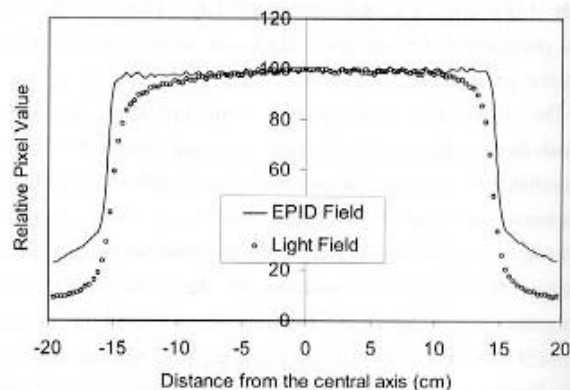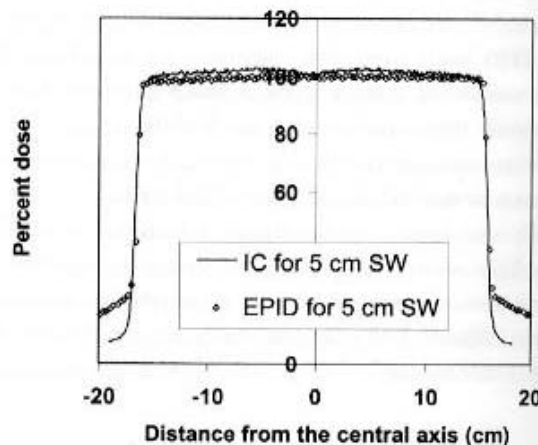Fig. 8 through 10 show that as the thickness of the homogeneous phantom increases, the data between penumbrae become more and more curved (the source-to-EPID distance is fixed at 161.9 cm). To avoid complicating the data presentation, these figures display the results in only selected solid-water thickness.

Fig. 8 through 10 show that as the thickness of the phantom increased, the EPID gave rise to relative over-response at beam axis.

Fig. 11 and 12 show that in the regions surrounding the lung and solid-water interfaces of two different heterogeneous phantoms, the EPID scan can deviate by as much as 7% from the ion-chamber scan.

DISCUSSION AND CONCLUSION

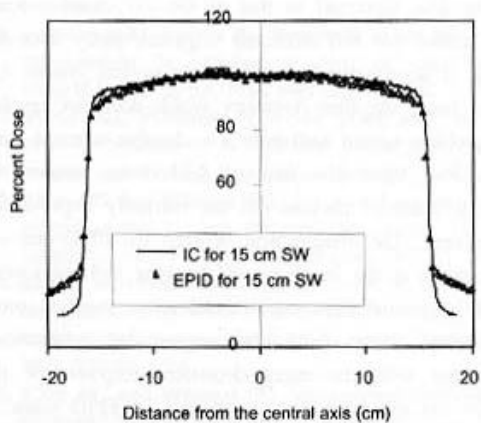The contributions of the energy-response of the

Fig. 9. EPID (diamonds) and ion-chamber (line) scans for a 15 cm-thick homogeneous phantom.
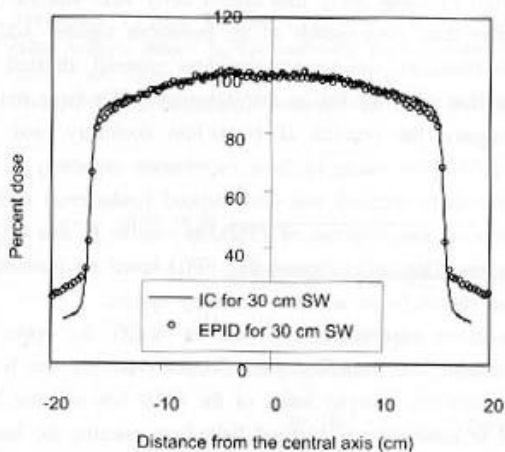

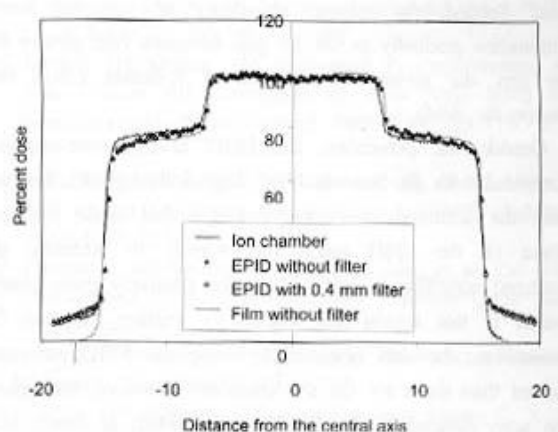Fig. 10. EPID (diamonds) and ion-chamber (line) scans for a 30 cm-thick homogeneous phantom.

Fig. 11. EPID and ion-chamber scans for heterogeneous phantom (lung density in the middle; see the first phantom in Fig. 3) with a total thickness of 15 cm. Thick line, ion chamber; triangles, EPID without filter; diamonds, EPID with 0.4 mm lead filter; thin line, film without filter.
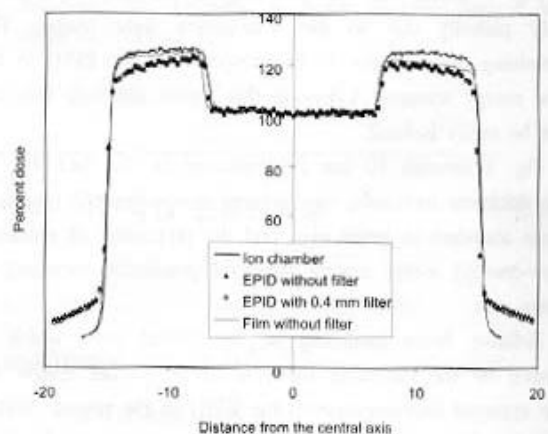

Fig. 12. EPID and ion-chamber scans for a heterogeneous phantom (lung density at the sides, see the second phantom in Fig. 3) with a total thickness of 15 cm. Thick line, ion chamber; triangles, EPID without filter; diamonds, EPID with 0.4 mm lead filter; thin line, film without filter.

detector and light scattering to the response of fluorescent screenbased EPID cannot be easily isolated from one another because light scattering is a systematic event that is always present. However, results obtained after varying the type of phantom used will provide some insight into the individual effect of scatter on EPID response. Using homogeneous phantoms will result in more uniform light scattering, thereby the effect of light scattering within the field should be minimal, whereas heterogeneous phantoms augment the effect of light scattering.

Regardless of the dosimetry system (ion chamber or EPID), the increase in the air gap causes the curves between the two penumbra regions flatten (Fig. 4 through 6). We feel that two factors contribute to the flattening of these curves. First, the scattered

x-rays emitted from the bottom of the homogeneous phantom are more abundant at beamaxis than off-axis. Because of this situation, the proportion of low energy x-rays (those with energies less than 400 keV) in the total population of x-ray photons is higest at beamaxis. Second, the relative abundance of scattered x-rays diminishes gradually as the air gap increases (the greater the air gap, the greater the number of scattered x-rays that escape the field).

Outside the penumbra, the EPID always

over-responds compared with the ion chamber (Fig. 4 through 6), because only the scattered (low energy) x-rays that cause over-response of the EPID reach this region. In addition, the scattered scintillation light will make relatively more contribution in this region (see Figure 7). Further, between the penumbrae, the data obtained by using the EPID are more curved than those for the ion chamber. Therefore, throughout the scan dimension, the EPID over-responds at beam axis, and this situatin is a consequence of the relative abundance of low energy x-rays at beam axis, as we mentioned previously. In addition, because of the increasing number of scattered x-rays that escape the field, the over-response of the EPID at beam axis decreases as the air gap increases.

Fig. 7 shows that the over-response outside the field is only partially due to the scintillation light scatter. The remaining is likely due to over-response of the EPID to the low energy scattered x-rays in this region although this can not be easily isolated.

Fig. 8 through 10 can be explained by the fact that as the thickness increases, the scattered x rays become relatively more abundant at beam axis, and the proportion of scattered(low energy) x-rays among the total population increases at beam axis.

Relative beam hardening at the central axis, which is caused by the flattening filter, is likely another reason for the apparent over-response of the EPID in the region. Within the first 5 to 10 cm into the phantom, we expect the dose profile between the penumbrae to flatten, due to the use of the flattening filter. At increased depths, the relative hardness of the primary beam at beam axis (compared to the beam at off-axis) causes lesser attenuation at the central axis. However, between penumbrae for the homogeneous phantom, all of the scans generated by using the EPID showed less than 5% error as compared to those obtained by using the ion chamber

The EPID scan can deviate by as mush as 7% from the ion-chamber scan as shown by Fig. 11 and 12. the large over-response of the EPID outside the penumbrae is not surprising in light of the factors we discussed previously. The shape of the EPID scan does not reflect as much change in dose (contrast) as that of the ion chamber scan, and we believe that this difference originates partly from the scattering of scintillation light within the optical system On the other hand, the film dosimetry which dose not involve such a problem agreed well with ion chmber scanned data. Using a lead filter (0.4mm or thicker) to remove the low energy, scattered photons did not markedly improve the EPID response. The disagreement between the EPID and ion chamber scans at the interfaces of the lung and solid-water are likely originated from experimental errors (such as setup reproducibility). These observations suggest that light scattering, together with the energy-dependent response of the EPID, are the important sources of error in EPID scans of heterogeneous phantoms.

Although film dosimetry showed some errors an asymmetry (as are typical of film densitometry), the scan obtained by using X-ray film agreed fairly well with the ion chamber data, even outside of the penumbra regions. Adding tissue-equivalent (solid-water) build-up material (instead of using film cassette) led to this agreement. We have further investigated the benefits of portal-film dosimetry, and we will publish the results of those demonstrated separately.

This study revealed and demonstrated fundamental characteristics of dose response of EPID, as relative to that of ion chambers. This study showed that EPID based on fluorescent screen cannot be an accurate dosimetry system.

In future experiments, We plan to modify the optics of the camera lens (including anti-reflective coatings), use better light absorbing material inside of the EPID box and use lens hood to minimize the scattered light from entering the lens.

ACKNOWLEGMENTS

REFERENCES

1. Boyer AL, Antonuk L, Fenster A., et al. A review of electronic portal imaging devices (EPIDs). Med Phys 1992; 19: 1-16

2. Heijmen BJM, Pasma KL, Kroonwijk M, et al. Portal dose measurement in radiotherapy using an electronic portal imaging device (EPID). Phys Med Biol 1995; 40, 1943-1955

3. Visser AG, Huizenga H, Althof VGM, and Swanenburg BN. Performance of a prototype fluoroscopic radiotherapy imaging system. Int J Radiat Oncol Biol Phys 1990; 18:43-50

4. Kirby MC and Williams PC. The use of an electronic portal imaging device for exit dosimetry and quality control measurements. Int J Radiat Oncol Biol Phys 1995; 31: 593-603

5. Essers M, Hoogervorst BR, van Herk M, Lanson H, and Mijnheer BJ. Dosimetric characteristics of a liquid-filled electronic portal imaging device. Int J Radiat Oncol Biol Phys 1995; 33:1265-1272

6. Kirby MC and Williams PC. Measurement possibilities using electronic portal imaging device. Radiother Oncol 1993; 29: 237-243

7. Zhu Y, Jiang X, and van Dyk J. Portal dosimetry using a liquid chamber matrix: Dose response studies. Med Phys 1995; 22:1101-1106

8. Yohannes Y, Yeo IJ, Guan H, and Zhu Y. Electronic portal imaging device (EPID) dosimetry: An experimental and Monte Carlo Study. Med Phys 1997; 24:1032

9. Wong JW, Slessinger ED, Hermes RE, et al. Portal dose images I : Quantitative treatment plan verification. Int J Radiat Oncol Biol Phys 1990; 18:1455-1463

10. McNutt TR, Mackie TR, Reckwerdt P, Papanikolaou N, and Paliwal BR. Calculation of portal dose using the convolution/superposition method. Med Phys 1996; 23: 527-535

11. van Dam J, Vaerman C, Blanckaert N, et al. Are port films reliable for in vivo exit dose measurement? Radiother Oncol 1992; 25:67-72

12. Fiorino C, del Vecchio A, Cattaneo GM, et al. Exit dose measurement by portal film dosimetry. Radiother Oncol 1993; 29:336-340

13. Attix FH. Introduction to Radiological Physics and Radiation Dosimetry. John Wiley & Sons, 1986

14. Jaffray DA, Battista JJ, Fenster A, and Munro P. X-ray scatter in megavoltage transmission radiography: Physical characteristics and influence on image quality. Med Phys 1994; 21:45-60

15. Burch SE, Kearfott KJ, Trueblood JH, et al. A new approach to film dosimetry for high energy photon beam: lateral scatter filtering. Med Phys 1997; 24:775-783

16. Yeo IJ, Wang CK, and Burch SE. A filtration method for improving film dosimetry in photon radiation therapy. Med Phys 1997;12:1943-1953

*

St. Jude Children's Research Hospial, Department of Radiation Oncology, Memphis. USA†

*, Yonas Yohannes, M.S. † and Yunping Zhu, Ph.D. †

____ :   .

_____:

                                                                        .

                              .

____ :   .

                                    7%   .

                              .

____ :   .

                              .

          :   ,   ,